A RESPONSIVE MYOELECTRIC CONTROL SIGNAL PROCESSING TECHNIQUE USING MUSCLE EXCITATION-CONTRACTION MODELING

Barathwaj Murali, MS[1] and Richard F. *ff.* Weir, PhD[1,2]

[1] Department of Bioengineering, University of Colorado Anschutz Medical Campus, Aurora CO USA, [2] Rocky Mountain Regional VA Medical Center, Aurora CO USA

ABSTRACT

Existing myoelectric controllers operate in a sequential fashion and use a state machine architecture to select grip postures. Direct control interfaces that seek to map individual muscles with joints in a prosthesis can provide a greater ability to perform individuated movements but require users to selectively activate their muscles to prevent unintended motion from natural muscle co-activations. Musculoskeletal modeling offers a possibility to estimate joint motion from muscle co-activation patterns themselves but require significant computational resources to run in real time. A major source of delay in a myoelectric system that reduces the amount of time available for advanced signal decoding schemes such as a musculoskeletal model is the low-pass filtering of rectified EMG signals. To minimize these delays, we explore the low-pass filtering properties of skeletal muscle using a simplified excitation-contraction dynamics model, applying a thresholded EMG signal and the rectified EMG profile itself as model inputs. Our results indicate that passing these signals through a biomechanical model of muscle can produce a usable myoelectric control signal while introducing a physiologically appropriate amount of delay between EMG onset and muscle force estimation.

INTRODUCTION

Approximately 541,000 individuals live with an upper limb deficiency in the United States [1]. Myoelectric control options for these individuals typically include two-site myo (the standard of care), pattern recognition, and postural control [2-4]. These systems operate in a sequential open-close fashion as users can switch between grip postures but are unable to modify their motions in real-time or combine postures simultaneously. The state machine architecture used by these controllers also reduces the capability of multi-articulated prosthetic hands to simple grasping mechanisms. Direct control schemes seek to achieve simultaneous joint motion using targeted EMG electrode placement to provide a greater number of control sites. Cipriani et al. [5] demonstrated the ability of intact individuals to produce individuated and simultaneous thumb, index, and middle finger motions through a direct control interface using intramuscular EMG measured from the extrinsic finger flexors. However, mapping joint motion to EMG activity produced by individual muscle compartments required users to selectively activate their targeted muscles and avoid producing natural muscle co-activations that play an important role in producing dexterous motions. Musculoskeletal simulation provides an appealing option to estimate joint motion produced by muscle co-activations that ultimately result in complex and intuitive limb motion.

Using a musculoskeletal model as a signal decoding interface requires significant computational overhead to run in real-time [6]. A real-time myoelectric control system must acquire, process, and decode EMG data at a rate faster a human operator can perceive. Users can largely tolerate controller update rates of 100ms before complaining of sluggish performance [7]. The low-pass filtering (or enveloping) of EMG activity can introduce delays between the onset of muscle contraction and prehensor motion ranging between 50-250ms [8]. Larger filtering time constants reduce the overall system bandwidth along with the proportion of the controller update rate available for more sophisticated signal decoding schemes. Childress et al. [9] developed a highly responsive control signal by thresholding the EMG amplitude profile and pulse modulating a motor within a myoelectric prehensor to leverage its inherent dynamics for low-pass filtering. Skeletal muscle performs a similar role in the body by producing a force response from pulsed motor unit action potentials that closely follows a minimum-jerk smoothness profile [10]. In this work, we apply a thresholded (or myopulse) EMG signal in addition to the rectified EMG amplitude profile as inputs to a physiological model of muscle excitation-contraction dynamics to demonstrate its ability to produce a smooth output response while introducing a physiologically appropriate delay between EMG onset and muscle contraction.

METHODS

Muscle Excitation-Contraction Dynamics

A simplified model of muscle excitation dynamics based on the model in Krylow et al. [10] consisted of two coupled first-order ODEs to estimate the active state of the muscle, defined as the rate at which calcium-bound troponin exposes actin binding sites for cross-bridge formation [11]. The amount of free calcium $r(t)$ in Eqn. 1 is proportional to pulsed input $x(t)$ and offset by the reabsorption of free calcium. The proportion of bound calcium $y(t)$ in Eqn. 2 provides the active state of the muscle, bounded between 0 and 1. The coefficients $C_1 = 100$, $C_2 = 107$, $C_3 = 99$, and $C_4 = 94$ were determined by fitting Eqns. 1 and 2 to match muscle activation and deactivation time constants of 10ms and 40ms recommended for human muscle [12].

$$\dot{r}(t) = C_1 x(t) - C_2 r(t) \tag{1}$$

$$\dot{y}(t) = \begin{cases} C_4 r(t) - C_3 y(t), & y(t) \le 1 \\ -C_3 y(t), & y(t) > 1 \end{cases} \tag{2}$$

The active state estimated by Eqn. 2 drove a simplified two-element model [10], illustrated in Figure 1a, consisting of a contractile element representing the muscle body and a series elastic element representing the tendon. The contractile element followed Hill's force-velocity relation [13], expressed in Eqn. 3

$$V_{CE} = \frac{b_0(P_0 y - F_M)}{F_M + a_0} \tag{3}$$

where V_{CE} is the muscle shortening velocity, $a_0 = 0.3$ and $b_0 = 0.04\ m/s$ are Hill model constants, $P_0 = 24.1\ N$ is the maximum isometric muscle force, F is the contractile element force, and y is the muscle active state [10].

The force developed by the series elastic tendon in Eqn. 4 is equal to contractile element force F_M and can be expressed in terms of total muscle length L_M and contractile element length L_{CE}

$$F_{SE} = kL_{SE} = k(L_M - L_{CE}) \tag{4}$$

where F_{SE} is the force on the tendon, $k = 1800\ N/m$ is the tendon stiffness [10], and L_{SE} is the tendon length.

Scaling the model constants a_0, b_0, and k using an empirical isometric force-length curve from Krylow et al. [10] introduces length-dependence to the force-velocity and tendon stiffness equations in Eqns. 3 and 4. Differentiating Eqn. 4 yields the ordinary differential equation governing contractile element force production

$$\frac{dF_M}{dt} = k(V_M - V_{CE}) \tag{6}$$

In Eqn. 6, the velocity of the muscle-tendon endpoint (V_M) is set to zero to represent an isometric force scenario. The system of ODEs formed by Eqns. 1-3 and 6 were solved using a fourth-order Runge-Kutta integrator.

Experimental Protocol

Eight subjects (6M/2F, all right-handed, age 28.6 ± 7.6 yrs.) performed a set of steady-state isometric contraction tasks consisting of a single isometric force trial at Maximum Voluntary Contraction (MVC) followed by a series of sub-maximal contraction tasks in increments of 20-percent MVC. Subjects provided informed consent for their participation and the protocol was approved by the Colorado Multiple Institutional Review Board (COMIRB). Subjects produced isometric forces by gripping a Jamar hand dynamometer instrumented with a pressure transducer (Honeywell, Charlotte NC) while a single differential electrode (Delsys, Natick MA) placed on the medial surface of the forearm recorded EMG activity from the extrinsic finger flexors. Data was acquired at 2000 Hz while a custom graphical interface developed provided visual cues of target grip force levels to participants.

Data Analysis

Surface EMG data was bandpass filtered (6th order Butterworth, 30 Hz high-pass, 480 Hz low-pass) and notch filtered (2nd order IIR bandstop, 60 Hz stopband frequency). After normalizing EMG data to MVC values for each subject, the myopulse signal was computed for each isometric force trial using a threshold value of three standard

deviations above the mean quiescent EMG amplitude. The muscle excitation-contraction dynamics model estimated muscle force using the myopulse signal and the rectified EMG amplitude profile as separate inputs. The average steady-state isometric forces estimated by the model were used to determine the relationship between estimated muscle force and measured muscle contraction level.

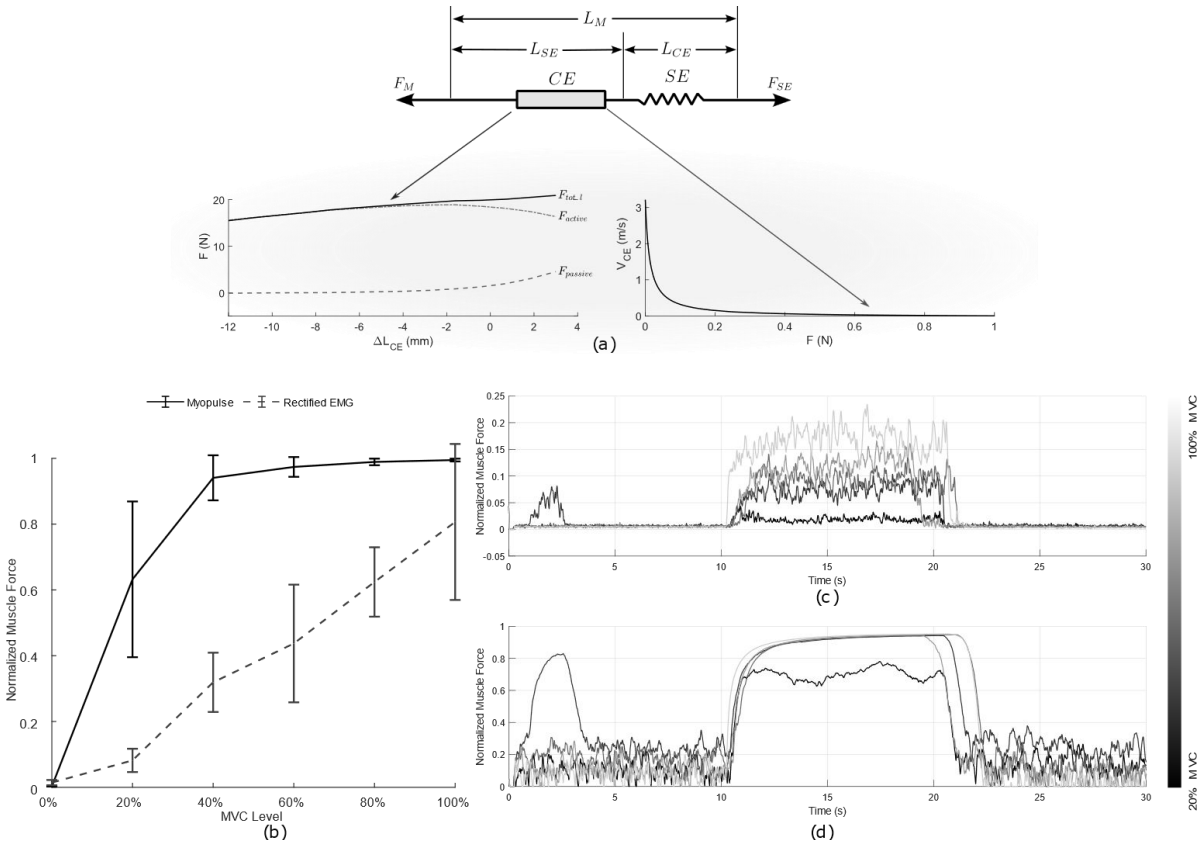

Figure 1: (a) Two-element Hill model from Krylow et al. [10] and force-length and force-velocity relations. (b) Normalized muscle forces plotted against steady state MVC contraction level. (c) Time series plot of estimated muscle forces from excitation-contraction dynamics model from rectified EMG signal. (d) Time series plot of estimated muscle forces from myopulse signal.

RESULTS

The forces estimated from the myopulse signal produced a hyperbolic relationship with muscle contraction level, (Figure 1b), while the forces estimated from rectified EMG amplitudes produced a linear relationship with muscle contraction level. The myopulse signal produced a smoother force response at steady-state isometric contraction levels and reached higher force magnitudes (Figure 1c), but also produced noisier forces during the quiescent portions of the isometric force trials. The opposite was true for the force profiles produced by the rectified EMG signal (Figure 1d) characterized by smoother quiescent forces and noisier steady state values.

DISCUSSION

We explored the ability of a physiological model of muscle excitation-contraction dynamics to avoid introducing large time constants associated with EMG low-pass filtering. The system of equations governing the model essentially act a cascaded fourth-order filter that successively smooths the input signal and constrains the delays introduced at each stage within a physiologically appropriate range. From Figure 1, the forces estimated from the quiescent myopulse signal are noisier than those estimated from the rectified EMG signal. This result is most likely due to the on-off nature of the myopulse signal which would cause noticeable force production depending on the time constants used by the excitation dynamics equations. In contrast, the rectified EMG signal produced a noisier steady-state force

profile but a smoother quiescent period. Since the rectified signal retains its amplitude information, the active state estimated from low EMG amplitudes will also be small in magnitude. Although the magnitudes of the estimated muscle forces vary between the myopulse and rectified EMG inputs, proper scaling and normalization will produce sufficient output signal magnitudes to drive a myoelectric system. The selection of excitation dynamics coefficients and tendon stiffness values influences the rise time of the muscle force profiles, as an inverse relationship exists between the amount of delay introduced to the output signal and the degree of smoothing performed by the excitation-contraction dynamics model.

The steep increase in output force produced by the myopulse signal at low muscle contraction levels and force saturation at higher contraction levels may be a result of the interaction between the force-velocity curve with the response of the myopulse signal with increasing muscle contraction. As these relationships are both hyperbolic but inverse to each other [9, 13], it is likely that these quantities cancel at higher MVC levels while remaining either linear or hyperbolic at lower contraction levels given a mismatch in slopes. Combining the myopulse and rectified EMG signals may produce an improved force response across all muscle contraction levels. Multiplying the myopulse signal with the rectified EMG signal would produce a thresholded signal that retains amplitude information. The corresponding muscle force behavior would most likely display high sensitivity at low contraction levels from the myopulse signal content and high linearity across contraction levels from the rectified EMG amplitudes.

CONCLUSION

We evaluated the ability of thresholded and rectified EMG data to produce a responsive myoelectric control signal using simplified model of muscle excitation-contraction dynamics. These results further confirm the physiological role of muscles as a biological low-pass filter and establish the ability of a muscle model to sufficiently filter rectified EMG activity while introducing physiologically appropriate delays to the output signal. Additionally, from observing the properties of the estimated force profiles produced using thresholded and rectified EMG signals, we believe that combining both signals will produce a robust myoelectric control signal that displays high sensitivity at lower contraction levels favorable to myoelectric control use while producing a linear response at higher contraction levels.

ACKNOWLEDGEMENTS

This work was supported by the National Science Foundation Graduate Research Fellowship (GRFP) Grant No. 230762.

REFERENCES

[1] K. Ziegler-Graham, E. J. MacKenzie, P. L. Ephraim, T. G. Travison, and R. Brookmeyer, "Estimating the Prevalence of Limb Loss in the United States: 2005 to 2050,", *Arch. Phys. M,* vol. 89, no. 3, pp. 422-429, 2008.

[2] J. L. Segil and R. F. f. Weir, "Novel postural control algorithm for control of multifunctional myoelectric prosthetic hands," *J Rehabil Res Dev,* vol. 52, no. 4, pp. 449-466, 2015.

[3] K. Englehart and B. Hudgins, "A robust, real-time control scheme for multifunction myoelectric control," (in en), *IEEE Transactions on Biomedical Engineering,* vol. 50, no. 7, pp. 848-854, 2003.

[4] N. Berger and C. R. Huppert, "The use of electrical and mechanical muscular forces for the control of an electrical prosthesis," (in eng), *Am J Occup Ther,* vol. 6, no. 3, pp. 110-114, 1952.

[5] C. Cipriani, J. L. Segil, J. A. Birdwell, and R. F. f. Weir, "Dexterous Control of a Prosthetic Hand Using Fine-Wire Intramuscular Electrodes in Targeted Extrinsic Muscles," *IEEE Trans Neural Syst Rehabil Eng,* vol. 22, no. 4, pp. 828-836, 2014.

[6] A. J. van den Bogert, D. Blana, and D. Heinrich, "Implicit methods for efficient musculoskeletal simulation and optimal control," *Procedia IUTAM,* vol. 2, pp. 297-316, 2011.

[7] T. R. Farrell and R. F. Weir, "The Optimal Controller Delay for Myoelectric Prostheses," *IEEE Trans Neural Syst Rehabil Eng,* vol. 15, no. 1, pp. 111-118, 2007.

[8] R. Merletti and P. Di Torino, "Standards for reporting EMG data," *J Electromyogr Kinesiol,* vol. 9, no. 1, pp. 3-4, 1999.

[9] D. S. Childress, D. W. Holmes, and J. N. Billock, "Ideas on myoelectric prosthetic systems for upper-extremity amputees," *The control of upper-extremity prostheses and orthoses,* pp. 86-106, 1974.

[10] A. M. Krylow and W. Z. Rymer, "Role of intrinsic muscle properties in producing smooth movements," *IEEE Transactions on Biomedical Engineering,* vol. 44, no. 2, pp. 165-176, 1997.

[11] A. M. Gordon, A. F. Huxley, and F. J. Julian, "The variation in isometric tension with sarcomere length in vertebrate muscle fibres," (in en), *The Journal of Physiology,* vol. 184, no. 1, pp. 170-192, 1966.

[12] F. E. Zajac, "Muscle and tendon: properties, models, scaling, and application to biomechanics and motor control," (in eng), *Crit Rev Biomed Eng,* vol. 17, no. 4, pp. 359-411, 1989.

[13] A. V. Hill, "The heat of shortening and the dynamic constants of muscle," *Proc. Roy. Soc.,* vol. B126, pp. 136-195, 1938.